ELSEVIER

Journal of Nuclear Materials 283–287 (2000) 545–550

journal of nuclear materials

www.elsevier.nl/locate/jnucmat

In situ thermal conductivity measurement of ceramics in a fast neutron environment

L.L. Snead [a,*], R. Yamada [b], K. Noda [b], Y. Katoh [c], S.J. Zinkle [a], W.S. Eatherly [a], A.L. Qualls [a]

[a] *Metals and Ceramics Division, Oak Ridge National Laboratory, P.O. Box 2008, MS-6087, Oak Ridge, TN 37830-6087, USA*
[b] *Japan Atomic Energy Research Institute, Tokai, Naka, Ibaraki 319-1195, Japan*
[c] *Kyoto University, Gokasho, Uji, Kyoto 611, Japan*

Abstract

A temperature controlled instrumented capsule has been irradiated in the RB* position of the high flux isotope reactor (HFIR) at the Oak Ridge National Laboratory in order to perform in situ thermal conductivity measurements of monolithic ceramics and composite materials during neutron irradiation. This determination of thermal conductivity utilizes a temperature gradient technique whereby two thermocouples measure the absolute temperature along a cylindrical sample which is constrained to one-dimensional thermal conduction. The heat source is the intrinsic gamma heating of the core region of the HFIR. This paper provides an overview of the experiment and gives preliminary results on the degradation in thermal conductivity of a few ceramic specimens measured as a function of irradiation temperature (200–700°C) and fast neutron fluence up to $\sim 3.4 \times 10^{25}$ n/m^2 ($E > 0.1$ MeV).

1. Introduction

Due to the low density of conduction band electrons in ceramic materials, the dominant path for thermal conduction is phonon transport. The temperature dependent thermal conductivity $K(T)$ can be written as the summation of phonon scattering terms, or thermal resistances, as follows [1–4]:

$$[K(T)]^{-1} = \left[\frac{1}{K_u(T)} + \frac{1}{K_{gb}(T)} + \frac{1}{K_{d0}}\right], \quad (1)$$

where $1/K_u(T)$ is the resistance due to phonon–phonon (umklapp) scattering, $1/K_{gb}$ the scattering due to grain boundaries, and $1/K_{d0}$ is the scattering due to defects such as dislocations, impurities, vacancies, etc. All of these thermal resistance terms have a strong temperature dependence at low temperatures (<300 K), but they exhibit a weak or simple temperature dependence above room temperature. For a high quality, low defect material, the grain boundary term becomes insignificant above room temperature. However, the umklapp term, which is proportional to temperature, dominates the thermal resistance for temperatures considered for ceramics of interest for fusion structural materials such as SiC (>500°C) or insulating breaks (>300°C.) The defect term can be considered as temperature independent for temperatures above room temperature.

The room temperature thermal conductivities of some non-irradiated ceramic materials can rival or exceed high conductivity metals such as pure copper. Examples include pyrolytic graphite (>1000 W/m K), silicon carbide (~490 W/m K), and beryllium oxide (~240 W/m K). The key to achieving such high thermal conductivities is to have as near to perfect a crystal as possible. While there is no way to mitigate the thermal resistance due to umklapp scattering, both the grain boundary and defect scattering terms can be significantly reduced by moving towards crystals with very low defect and impurity densities.

The sensitivity of thermal conductivity to point defects makes this property acutely affected by neutron

* Corresponding author. Tel.: +1-423 574 9942; fax: +1-423 576 8424.
E-mail address: z2n@ornl.gov (L.L. Snead).

0022-3115/00/$ - see front matter
PII: S0022-3115(00)00237-3

irradiation. Since the mobility of point defects and the spontaneous point defect recombination volume in most ceramics are quite low as compared to metals [5,6], fast neutron damage can produce large populations of stable simple defects and defect clusters in ceramics. These defects have been shown to reduce the room temperature thermal conductivity by orders of magnitude for graphite [7–13], silicon carbide [14–18] and a range of other ceramics and glasses after neutron irradiation near room temperature to doses $\ll 1$ dpa.

Due to the dramatic effect of neutron irradiation on the thermal transport in ceramic in general, and in particular the need to examine new, improved ceramic composites an experiment was carried out to provide engineering information on irradiated ceramics and composites for conditions relevant to fusion energy. Furthermore, by using an in situ approach to measuring this thermal conductivity, data are generated real time from the very low fluence where most of the degradation in thermal conductivity takes place out to fluence levels associated with saturation in thermal conductivity. With this fundamental knowledge it is expected that models can be constructed for prediction of thermal conductivity degradation of future, higher thermal conductivity structural ceramics.

2. Experimental

2.1. Materials and measurement method

The temperature regulated in situ testing–thermal conductivity (TRIST–TC1) experiment was segmented into three separate heat-controlled zones with nominal temperatures of ~200°C, ~400°C and ~700°C. Two 0.5-mm diameter Type N thermocouples were brazed onto opposite ends of a cylindrical sample to measure the ΔT between them. One end of the sample was brazed to a heat sink. Specimens were machined to be a 6-mm outside diameter solid cylinders whose lengths varied dependent on the estimated irradiated thermal conductivity to produce an estimated temperature difference of ~40°C between the thermocouples at the end of irradiation. Fig. 1 shows a sub-capsule assembly with two samples brazed onto a vanadium alloy holder. Each sample shows a 0.76-mm deep hole drilled into the free end into which a 'hot' thermocouple is brazed. A second 'cold' thermocouple is passed through a slot in the vanadium holder base and brazed into a similar hole at the heat sink end (not shown). Thermal conductivity of these specimens was calculated using the temperature difference ΔT using a three-dimensional thermal transport code taking into account loss of heat to thermocouples and conduction to capsule gas environment. Heat generation due to nuclear heating was assumed to be constant within the sample.

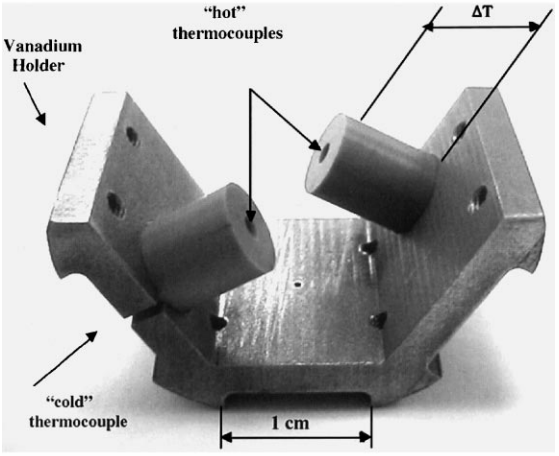

Fig. 1. Photograph of TRIST–TC1 assembly holding two cylindrical samples.

Forty specimens, in addition to eight F82H 'control' specimens were split between the three temperature zones. Specifics related to these materials including the axial position in their capsule are given in Table 1. In some cases the assumed room temperature thermal conductivity, primarily based on manufacturer' supplied information, is given. Additional information regarding the assembly details for this capsule is described by Qualls [19] elsewhere in this proceedings.

2.2. Irradiation

The TRIST–TC1 capsule was placed into the RB* position prior to cycle start-up of the high flux isotope reactor (HFIR) and irradiated for three reactor cycles. The total peak flux in this position is estimated to be 6×10^{18} n/m^2 s ($E > 0.1$ MeV) yielding a peak dose over the 66 full power days irradiation of approximately 3.4 dpa in SiC. The actual dose for each sample will depend on location in the capsule due to axial flux variation. Between the second and third cycles the capsule was rotated 180° which slightly changed the distance from the reactor fuel thereby changing the nuclear heating rate.

3. Results and discussion

Shown in Fig. 2 is an example of the temperature rise at the 'hot end' of a Morton CVD SiC sample in intermediate temperature Zone A (~400°C) as the reactor was brought on line for the first TRIST–TC1 irradiation cycle. Due to small adjustments in temperature controlling gas flow into the capsule there are many small fluctuations in the sample temperature during start-up.

Table 1
Materials, location and material properties

Material	Position	Temperature (°C)			Vendor and grade
		200	400	700	
FH2H (standard)	2, 515, 22, 28, 34, 39, 45	1	3	4	NKK (IEA) Heat
CVD SiC (Hi TC)	11, 20, 21, 42	1	2	1	Morton CVD ($K_{th}^{rt} \sim 400$ W/m K)
CVD SiC (Lo TC)	17, 30, 41	1	1	1	CVD SiC ($K_{th}^{rt} \sim 110$ W/m K)
Single X SiC	19		1		Cree Systems 6H-Alpha
3D SiC/SiC	6, 31		1	1	Kawasaki PIP 3D, Hi-Nicalon fiber
Non-woven SiC/SiC	8, 1		1	1	Mitsui CVI, Hi-Nicalon Type-S fiber
2D SiC/SiC, in-plane	7, 9[a], 29		2	1	ORNL FCVI, Satin Weave Nicalon-Type S
2D SiC/SiC, cross-plane	10, 27		1	1	ORNL FCVI, Satin Weave Nicalon-Type S
2D SiC/SiC	16, 25		1	1	MER CVR,CVR T-300 PAN Fiber
SiC-doped CFC	13, 32		1	1	Tonen ($K_{th}^{rt} \sim 410$ W/m K)
1D CFC	12		1		Mitsubishi MFC-1($K_{th}^{rt} \sim 560$ W/m K)
1D CFC	18, 26		1	1	Tonen ($K_{th}^{rt} \sim 495$ W/m K)
2D CFC	1, 23		1	1	FMI-222 ($K_{th}^{rt} \sim 200$ W/m K)
Graphite	14, 24		1	1	Segri-Great Lakes H451
Sapphire	4, 37, 48	1	1	1	Crystal Systems Hemlux Ultra (VUV)
Silicon nitride	38, 46	1		1	Kyocera SN235P
Beryllium oxide	3, 36, 44	1	1	1	Brush Wellman 995
Aluminum nitride	35, 43	1		1	Tokuyama SH15
Spinel	40, 47	1		1	Commercial Crystal Systems $MgAl_2O_3$

[a] Sample oxidized for 24 h at 600°C.

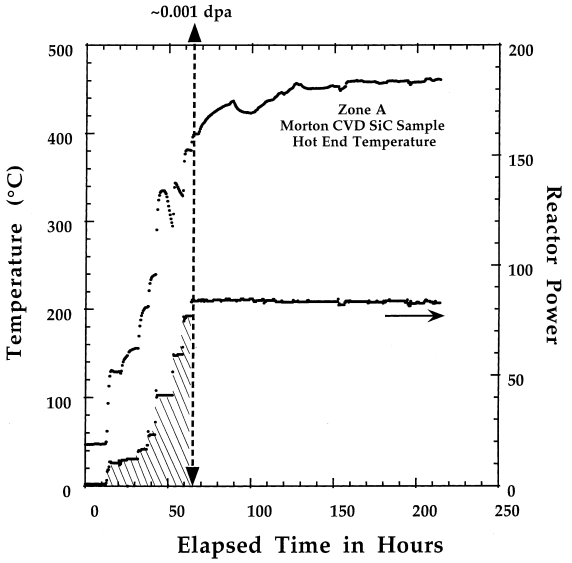

Fig. 2. Temperature at hot end of CVD SiC sample as a function of time (dose).

However, the temperature of the sample thermocouple generally tracks with increasing reactor power until full 85 MW operation is reached. At this point, the reactor power remains constant (dashed line in Fig. 2) while a small rise in sample temperature continues to occur. During the power start-up transient the samples received approximately 0.001 dpa at temperatures ranging from reactor coolant temperature (~60°C) up to the zone design temperature. This accumulation of dose at low temperature is especially important for relatively 'defect free' high thermal conductivity and has been demonstrated with post irradiation measurements on identical materials to those irradiated in this study. For example, the room temperature thermal conductivity Morton CVD SiC is seen to decrease from ~245 to 125 W/m K following a 0.001 dpa irradiation at ~60°C [6].

Fig. 3 gives examples of the cold and hot thermocouple measurements for two silicon carbide composites during and shortly after reactor start-up. As in Fig. 2, the sample temperature is seen to increase with increasing reactor power. During the reactor power 'hold' periods prior to full power the sample temperatures are seen to increase and then rapidly decrease. Temperature fluctuations on the order of 10°C also occurred after the reactor reached steady-state, full-power operation. These fluctuations were due to manipulation of the He/Ne/Ar gas mixture within the capsule responsible for heat conduction away from the sample holders. As shown in Fig. 3, and consistent with all samples studied, the thermocouple measurements tracked very closely with each other and showed evidence of small thermal turbulence within the subcapsules. In some cases, as seen at 150 min into the irradiation (Fig. 3), a small change in reactor power was responsible for a dip in the sample

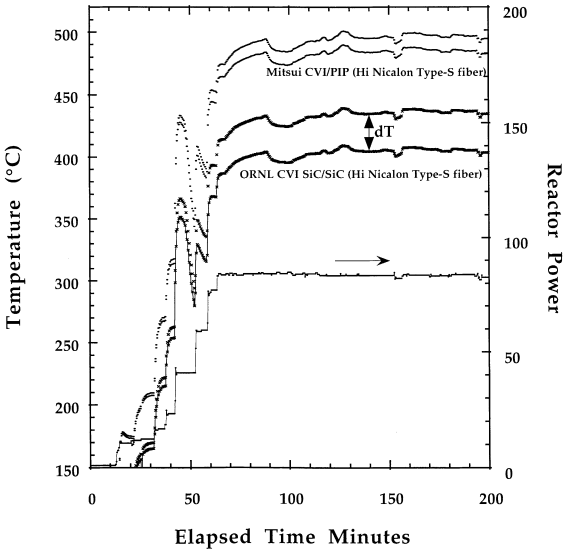

Fig. 3. Example thermocouple readings during reactor start-up.

temperature. The temperature history through the first, second and majority of the third cycle irradiation is given in Fig. 4 for the same materials given in Fig. 3. Of note is that the temperature difference, ΔT, increases for both samples during the early period of the first cycle and then stabilizes indicating that the thermal conductivity underwent rapid reduction followed by saturation. In addition to the thermal conductivity degradation, sample temperature is affected by the variation in gamma heating in the reactor core during the irradiation. This is especially true near the start and end of each reactor cycle due to the motion on the control plates.

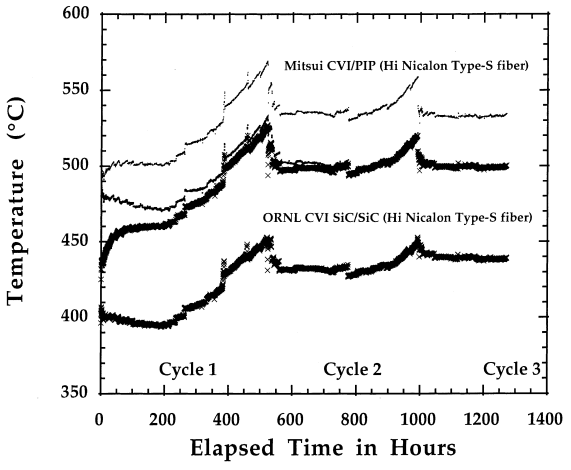

Fig. 4. Example thermocouple readings throughout 3-cycle irradiation.

Presently, it is difficult to give accurate information on the absolute thermal conductivity degradation for the materials in this experiment. This is partially due to uncertainties in the gamma heating measured by the F82H ferritic martensitic steel control specimens, as discussed elsewhere by Qualls [19]. Final analysis will also require a complete post-irradiation examination including an ex situ thermal conductivity measurement and inspection of the thermocouple braze joints. However, an example of the irradiation-induced thermal conductivity reduction for the high-purity Morton CVD SiC is shown in Figs. 5 and 6. Fig. 5 shows the estimated thermal conductivity during, and in the first hours following reactor start-up for the three temperature zones. In each case the mean temperature of the two sample thermocouples is given as a range which increased from beginning to end of the full power irradiation. For the calculation of Figs. 5 and 6, a gamma heating rate based on previous experiments and calculations [20] was used. Prior to reactor full power the gamma heating used for the thermal conductivity calculation was a value normalized to the full power value. Due to the significant spatial fluctuations associated with initial reactor start-up, it is expected that normalizing the gamma heating in this manner becomes unreliable at the lower reactor power levels.

While it is difficult to draw conclusions from the preliminary data of Figs. 5 and 6 a few observations can be made. The Morton CVD SiC used in this study had a room temperature thermal conductivity of ~245 W/m K in the non-irradiated condition (based on pre-irradiation measurement.) Taking into account the typical reduction in thermal conductivity due to

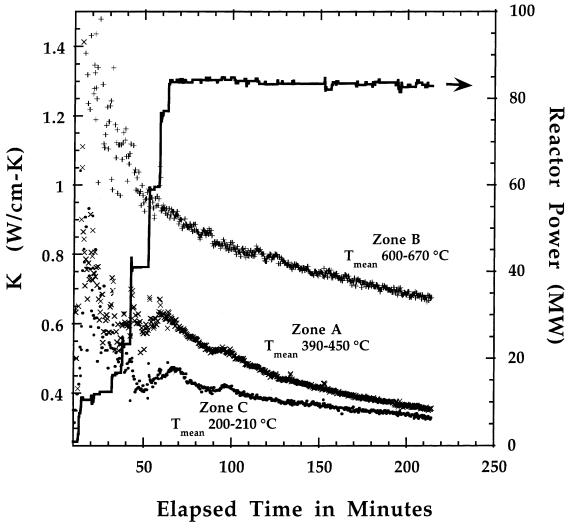

Fig. 5. Preliminary thermal conductivity estimate for Morton CVD SiC during start-up.

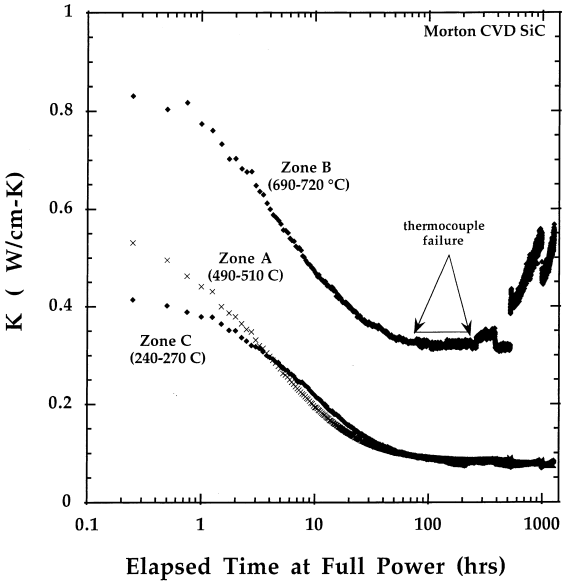

Fig. 6. Preliminary thermal conductivity estimate for Morton CVD SiC throughout 3-cycle irradiation.

umklapp scattering at the measurement temperature (of Fig. 5), it appears that by the time the reactor attained full power, a considerable reduction in thermal conductivity had already occurred for the Morton CVD SiC. Furthermore, the reduction appears to be more dramatic for the CVD SiC irradiated at lower temperature. As the full power operation continues, Fig. 5 clearly shows an additional steady decrease in thermal conductivity during the first few hours of full power operation. As the irradiation was carried out to higher doses, all three materials appeared to reach a saturation thermal conductivity by about 100 h (~0.2 dpa). Interestingly, the saturation thermal conductivity values were very similar for the ~200°C and ~420°C irradiation, though is substantially less than the ~635°C irradiated material.

Several of the 96 thermocouples used to measure the thermal conductivity in this experiment failed at some point during the irradiation. The unusual variations in thermal conductivity shown in Fig. 6 indicates a failure of unknown origin which occurred in the tip thermocouple for the high temperature zone Morton CVD SiC sample at about 70 h. In this case the tip thermocouple began to read successively lower values during the second half of the first cycle. During the third cycle, a discontinuity in the data occurred possibly indicating that the braze joint for the tip thermocouple had become compromised. This was one type of failure which occurred either immediately or during the course of the experiment. In other cases, the thermocouple wires themselves separated.

3.1. Concluding remarks

An experimental technique for measuring in situ the changing thermal conductivity values of ceramic materials as they accumulate irradiation damage in a high flux nuclear reactor was successfully demonstrated. The technique is based on measurement of the temperature drop along the axis of a solid cylinder constrained to one-dimensional heat flow. Preliminary results indicated that, as expected, the thermal conductivity of most ceramic materials undergo a rapid reduction in thermal conductivity with irradiation followed by an apparent saturation. Final results will be obtained after a detailed post-irradiation examination of the samples.

Acknowledgements

The authors would like to thank Dennis Heatherly and Bob Sitterson for their help with construction of this capsule and Jim King for assistance with the brazing development. This work has been carried out under the US DOE/JAERI Collaborative Program on Testing FWB Structural Materials in Mixed-Spectrum Fission Reactors, PhaseIII. This work was conducted for the Department of Energy Office of Fusion Energy by members of the Lockheed Martin Energy Research Corporation under contract DE-AS05-960OR22464.

References

[1] P.G. Klemens, in: F. Seitz, D. Turnbull (Eds.), Solid State Physics, vol. 7, Academic, New York, 1958, p. 1.
[2] P.G. Klemens, in: R.P. Tye (Ed.), Thermal Conductivity, vol. 1, Academic, New York, 1969, p. 1.
[3] D.R. Flynn, in: J.B. Wachtman Jr. (Ed.), Proceedings of the Symposium on Mechanical and Thermal Properties of Ceramics, NBS Spec. Publ. 303, National Bureau of Standards, Washington, DC, 1969, p. 63.
[4] B.T. Kelly, in: P.L. Walker (Ed.), Chemistry and Physics of Carbon, vol. 5, Marcel Dekker, New York, 1969, p. 119.
[5] H. Trinkaus, Mater. Sci. Forum 248&249 (1997) 3.
[6] S.J. Zinkle, L.L. Snead, unpublished.
[7] J.W.H. Simmons, Radiation Damage in Graphite, vol. 102, Pergamon, New York, 1965.
[8] B.A. Thiele, L. Binkele, K. Koizlik, H. Nickel, in: Proceedings of the 16th International Symposium on Effects of Radiation on Materials, ASTM, 1992.
[9] T. Maruyama, M. Harayama, J. Nucl. Mater. 195 (1992) 44.
[10] C.H. Wu, J.P. Bonal, B. Thiele, J. Nucl. Mater. 212–215 (1994) 1168.
[11] T.D. Burchell, W.P. Eatherly, J. Nucl. Mater. 179–181 (1991) 205.
[12] L.L. Snead, T.D. Burchell, J. Nucl. Mater. 224 (1995) 222.
[13] M. Eto et al., J. Nucl. Mater. 212–215 (1994) 1223.
[14] W. Dienst et al., J. Nucl. Mater. 174 (1990) 102.

[15] C.W. Lee, F.J. Pineau, J.C. Corelli, J. Nucl. Mater. 108&109 (1982) 678.
[16] J.C. Corelli, J. Hoole, J. Lazzaro, C.W. Lee, J. Am. Ceram. Soc. 66 (1983) 529.
[17] R.J. Price, J. Nucl. Mater. 46 (1973) 268.
[18] G.W. Hollenberg et al. J. Nucl. Mater. 219 (1995) 70.
[19] A.L. Qualls et al., presented at 9th Int. Conf. on Fusion Reactor Materials (ICFRM-9), Colorado Springs, CO, Oct. 1999.
[20] I.I Siman-Tov, Fusion reactor materials, Semiannual Progress Report, period ending 31 March 1987, 1987, p. 10.